Radboud Repository

Radboud University Nijmegen

PDF hosted at the Radboud Repository of the Radboud University Nijmegen

The following full text is a preprint version which may differ from the publisher's version.

For additional information about this publication click this link.
http://hdl.handle.net/2066/124550

Please be advised that this information was generated on 2021-10-18 and may be subject to change.

EUROPEAN ORGANISATION FOR NUCLEAR RESEARCH

CERN-PPE/94-206
14 December, 1994

Observations of π-B charge-flavor correlations and resonant Bπ and BK production

The OPAL Collaboration

Abstract

Evidence is presented for kinematic and charge correlations of B mesons with charged pions and kaons. Using a new technique, a sample of over 80 000 partially reconstructed B mesons is obtained in $3.5 \cdot 10^6$ hadronic Z^0 decays recorded using the OPAL detector at LEP. The invariant mass distributions of $B^+\pi^-$ and B^+K^- combinations show enhancements consistent with the decays of P-wave resonances of a b antiquark and a light quark. We observe an excess of $1\,738 \pm 195$ $B^+\pi^-$ pairs with invariant masses in the range 5.60-5.85 GeV and an excess of 149 ± 31 B^+K^- pairs with invariant masses in the range 5.80-6.00 GeV. Labeling the observed enhancements generically as B^{**} we find

$$\frac{\mathrm{BR}(Z^0 \to \bar{b} \to B^{**0} \to B^{(*)+}\pi^-)}{\mathrm{BR}(Z^0 \to \bar{b} \to B^+)} = 0.18 \pm 0.04\,,$$

$$\frac{\mathrm{BR}(Z^0 \to \bar{b} \to B_s^{**0} \to B^{(*)+}K^-)}{\mathrm{BR}(Z^0 \to \bar{b} \to B^+)} = 0.026 \pm 0.008\,,$$

where $B^{(*)+}$ indicates the sum of B^+ and B^{*+} and the errors include statistical and systematic contributions. From a study of π-B charge-flavor correlations we conclude that the production flavor of a B meson can be tagged with the charge of a pion in an appropriately chosen kinematic region, and that the performance of this flavor tag compares favorably in the $Z^0 \to q\bar{q}$ environment with lepton-based tags.

(Submitted to Z. für Physik C)

The OPAL Collaboration

R. Akers[16], G. Alexander[23], J. Allison[16], K. Ametewee[25], K.J. Anderson[9], S. Arcelli[2], S. Asai[24], A. Astbury[28], D. Axen[29], G. Azuelos[18,a], A.H. Ball[17], E. Barberio[26], R.J. Barlow[16], R. Bartoldus[3], J.R. Batley[5], G. Beaudoin[18], A. Beck[23], G.A. Beck[13], C. Beeston[16], T. Behnke[27], K.W. Bell[20], G. Bella[23], S. Bentvelsen[8], P. Berlich[10], S. Bethke[32], O. Biebel[32], I.J. Bloodworth[1], P. Bock[11], H.M. Bosch[11], M. Boutemeur[18], S. Braibant[12], P. Bright-Thomas[25], R.M. Brown[20], A. Buijs[8], H.J. Burckhart[8], R. Bürgin[10], C. Burgard[27], N. Capdevielle[18], P. Capiluppi[2], R.K. Carnegie[6], A.A. Carter[13], J.R. Carter[5], C.Y. Chang[17], C. Charlesworth[6], D.G. Charlton[8], S.L. Chu[4], P.E.L. Clarke[15], J.C. Clayton[1], S.G. Clowes[16], I. Cohen[23], J.E. Conboy[15], M. Cuffiani[2], S. Dado[22], C. Dallapiccola[17], G.M. Dallavalle[2], C. Darling[31], S. De Jong[12], L.A. del Pozo[8], H. Deng[17], M. Dittmar[4], M.S. Dixit[7], E. do Couto e Silva[12], J.E. Duboscq[8], E. Duchovni[26], G. Duckeck[8], I.P. Duerdoth[16], U.C. Dunwoody[5], P.A. Elcombe[5], P.G. Estabrooks[6], E. Etzion[23], H.G. Evans[9], F. Fabbri[2], B. Fabbro[21], M. Fanti[2], P. Fath[11], M. Fierro[2], M. Fincke-Keeler[28], H.M. Fischer[3], P. Fischer[3], R. Folman[26], D.G. Fong[17], M. Foucher[17], H. Fukui[24], A. Fürtjes[8], P. Gagnon[6], A. Gaidot[21], J.W. Gary[4], J. Gascon[18], N.I. Geddes[20], C. Geich-Gimbel[3], S.W. Gensler[9], F.X. Gentit[21], T. Geralis[20], G. Giacomelli[2], P. Giacomelli[4], R. Giacomelli[2], V. Gibson[5], W.R. Gibson[13], J.D. Gillies[20], J. Goldberg[22], D.M. Gingrich[30,a], M.J. Goodrick[5], W. Gorn[4], C. Grandi[2], E. Gross[26], J. Hagemann[27], G.G. Hanson[12], M. Hansroul[8], C.K. Hargrove[7], P.A. Hart[9], M. Hauschild[8], C.M. Hawkes[8], E. Heflin[4], R.J. Hemingway[6], G. Herten[10], R.D. Heuer[8], J.C. Hill[5], S.J. Hillier[8], T. Hilse[10], P.R. Hobson[25], D. Hochman[26], A. Höcker[3], R.J. Homer[1], A.K. Honma[28,a], R. Howard[29], R.E. Hughes-Jones[16], P. Igo-Kemenes[11], D.C. Imrie[25], A. Jawahery[17], P.W. Jeffreys[20], H. Jeremie[18], M. Jimack[1], M. Jones[6], R.W.L. Jones[8], P. Jovanovic[1], C. Jui[4], D. Karlen[6], J. Kanzaki[24], K. Kawagoe[24], T. Kawamoto[24], R.K. Keeler[28], R.G. Kellogg[17], B.W. Kennedy[20], B. King[8], J. King[13], J. Kirk[29], S. Kluth[5], T. Kobayashi[24], M. Kobel[10], D.S. Koetke[6], T.P. Kokott[3], S. Komamiya[24], R. Kowalewski[8], T. Kress[11], P. Krieger[6], J. von Krogh[11], P. Kyberd[13], G.D. Lafferty[16], H. Lafoux[8], R. Lahmann[17], W.P. Lai[19], J. Lauber[8], J.G. Layter[4], P. Leblanc[18], P. Le Du[21], A.M. Lee[31], E. Lefebvre[18], D. Lellouch[26], C. Leroy[18], J. Letts[4], L. Levinson[26], Z. Li[12], F. Liu[29], S.L. Lloyd[13], F.K. Loebinger[16], G.D. Long[17], B. Lorazo[18], M.J. Losty[7], X.C. Lou[8], J. Ludwig[10], A. Luig[10], M. Mannelli[8], S. Marcellini[2], C. Markus[3], A.J. Martin[13], J.P. Martin[18], T. Mashimo[24], W. Matthews[25], P. Mättig[3], U. Maur[3], J. McKenna[29], T.J. McMahon[1], A.I. McNab[13], F. Meijers[8], F.S. Merritt[9], H. Mes[7], A. Michelini[8], R.P. Middleton[20], G. Mikenberg[26], D.J. Miller[15], R. Mir[26], W. Mohr[10], A. Montanari[2], T. Mori[24], M. Morii[24], U. Müller[3], B. Nellen[3], B. Nijjhar[16], S.W. O'Neale[1], F.G. Oakham[7], F. Odorici[2], H.O. Ogren[12], C.J. Oram[28,a], M.J. Oreglia[9], S. Orito[24], J.P. Pansart[21], G.N. Patrick[20], M.J. Pearce[1], P.D. Phillips[16], J.E. Pilcher[9], J. Pinfold[30], D. Pitman[28], D.E. Plane[8], P. Poffenberger[28], B. Poli[2], A. Posthaus[3], T.W. Pritchard[13], H. Przysiezniak[18], M.W. Redmond[8], D.L. Rees[8], D. Rigby[1], M. Rison[5], S.A. Robins[13], D. Robinson[5], N. Rodning[30], J.M. Roney[28], E. Ros[8], A.M. Rossi[2], M. Rosvick[28], P. Routenburg[30], Y. Rozen[8], K. Runge[10], O. Runolfsson[8], D.R. Rust[12], M. Sasaki[24], C. Sbarra[2], A.D. Schaile[8], O. Schaile[10], F. Scharf[3], P. Scharff-Hansen[8], P. Schenk[4], B. Schmitt[3], M. Schröder[12], H.C. Schultz-Coulon[10], P. Schütz[3], M. Schulz[8], C. Schwick[27], J. Schwiening[3], W.G. Scott[20], M. Settles[12], T.G. Shears[5], B.C. Shen[4], C.H. Shepherd-Themistocleous[7], P. Sherwood[15], G.P. Siroli[2], A. Skillman[16], A. Skuja[17], A.M. Smith[8], T.J. Smith[28], G.A. Snow[17], R. Sobie[28], S. Söldner-Rembold[10], R.W. Springer[30], M. Sproston[20], A. Stahl[3], M. Starks[12], C. Stegmann[10], K. Stephens[16], J. Steuerer[28], B. Stockhausen[3], D. Strom[19], P. Szymanski[20],

R. Tafirout[18], H. Takeda[24], T. Takeshita[24], P. Taras[18], S. Tarem[26], M. Tecchio[9], P. Teixeira-Dias[11], N. Tesch[3], M.A. Thomson[15], O. Tousignant[18], S. Towers[6], M. Tscheulin[10], T. Tsukamoto[24], A. Turcot[9], M.F. Turner-Watson[8], P. Utzat[11], R. Van Kooten[12], G. Vasseur[21], P. Vikas[18], M. Vincter[28], A. Wagner[27], D.L. Wagner[9], C.P. Ward[5], D.R. Ward[5], J.J. Ward[15], P.M. Watkins[1], A.T. Watson[1], N.K. Watson[7], P. Weber[6], P.S. Wells[8], N. Wermes[3], B. Wilkens[10], G.W. Wilson[27], J.A. Wilson[1], V-H. Winterer[10], T. Wlodek[26], G. Wolf[26], S. Wotton[11], T.R. Wyatt[16], A. Yeaman[13], G. Yekutieli[26], M. Yurko[18], V. Zacek[18], W. Zeuner[8], G.T. Zorn[17].

[1]School of Physics and Space Research, University of Birmingham, Birmingham B15 2TT, UK
[2]Dipartimento di Fisica dell' Università di Bologna and INFN, I-40126 Bologna, Italy
[3]Physikalisches Institut, Universität Bonn, D-53115 Bonn, Germany
[4]Department of Physics, University of California, Riverside CA 92521, USA
[5]Cavendish Laboratory, Cambridge CB3 0HE, UK
[6]Carleton University, Department of Physics, Colonel By Drive, Ottawa, Ontario K1S 5B6, Canada
[7]Centre for Research in Particle Physics, Carleton University, Ottawa, Ontario K1S 5B6, Canada
[8]CERN, European Organisation for Particle Physics, CH-1211 Geneva 23, Switzerland
[9]Enrico Fermi Institute and Department of Physics, University of Chicago, Chicago IL 60637, USA
[10]Fakultät für Physik, Albert Ludwigs Universität, D-79104 Freiburg, Germany
[11]Physikalisches Institut, Universität Heidelberg, D-69120 Heidelberg, Germany
[12]Indiana University, Department of Physics, Swain Hall West 117, Bloomington IN 47405, USA
[13]Queen Mary and Westfield College, University of London, London E1 4NS, UK
[15]University College London, London WC1E 6BT, UK
[16]Department of Physics, Schuster Laboratory, The University, Manchester M13 9PL, UK
[17]Department of Physics, University of Maryland, College Park, MD 20742, USA
[18]Laboratoire de Physique Nucléaire, Université de Montréal, Montréal, Quebec H3C 3J7, Canada
[19]University of Oregon, Department of Physics, Eugene OR 97403, USA
[20]Rutherford Appleton Laboratory, Chilton, Didcot, Oxfordshire OX11 0QX, UK
[21]CEA, DAPNIA/SPP, CE-Saclay, F-91191 Gif-sur-Yvette, France
[22]Department of Physics, Technion-Israel Institute of Technology, Haifa 32000, Israel
[23]Department of Physics and Astronomy, Tel Aviv University, Tel Aviv 69978, Israel
[24]International Centre for Elementary Particle Physics and Department of Physics, University of Tokyo, Tokyo 113, and Kobe University, Kobe 657, Japan
[25]Brunel University, Uxbridge, Middlesex UB8 3PH, UK
[26]Particle Physics Department, Weizmann Institute of Science, Rehovot 76100, Israel
[27]Universität Hamburg/DESY, II Institut für Experimental Physik, Notkestrasse 85, D-22607 Hamburg, Germany
[28]University of Victoria, Department of Physics, P O Box 3055, Victoria BC V8W 3P6, Canada
[29]University of British Columbia, Department of Physics, Vancouver BC V6T 1Z1, Canada
[30]University of Alberta, Department of Physics, Edmonton AB T6G 2J1, Canada
[31]Duke University, Dept of Physics, Durham, NC 27708-0305, USA
[32]Technische Hochschule Aachen, III Physikalisches Institut, Sommerfeldstrasse 26-28, D-52056

Aachen, Germany

[a]Also at TRIUMF, Vancouver, Canada V6T 2A3

1 Introduction

The existence of significant charge correlations between weakly decaying B mesons and charged pions produced in $\bar{b}$ fragmentation could provide an important tool for the experimental investigation of CP violation in B decays [1]. Many promising channels for studying CP violation in B decays require tagging the initial flavor of a neutral B meson. Pions produced in the $\bar{b}$ fragmentation may provide a useful tag of the initial B flavor. An advantage of such a tag is that it uses no information from the hadron containing the b produced in association with the $\bar{b}$, and is thus complementary to other methods of flavor tagging.

The presence of narrow resonant states of a $\bar{b}$ and a light quark would enhance the performance of such a tagging method. Resonant P-wave states have been observed in the charm system [2, 3], raising the prospect of similar excited meson production in beauty hadronization. Calculations based on heavy quark effective theory [4] predict that two of the four lowest-lying P-wave states in heavy-light systems (both beauty and charm) should have intrinsic widths of approximately 20 MeV; studies of charm seem to bear out this prediction [2, 3]. The two remaining states are expected to be more than 400 MeV wide [5].

A large statistics sample of b hadrons is used to study Bπ charge and kinematic correlations and to search for resonant states. No effort is made to reconstruct exclusive final states of weakly decaying b hadrons; rather, an inclusive reconstruction is performed. Starting from a reconstructed secondary vertex well separated from the primary event vertex, the direction and energy of the weakly decaying b hadron are estimated. The charge of the decaying b hadron can also be estimated, allowing some separation between charged and neutral b hadrons. The resolution in the invariant Bπ mass is poorer than would result from using fully reconstructed B decays, but is adequate to distinguish between relatively narrow ($\Gamma < 50$ MeV) and broad states.

We study the kinematic properties (invariant mass and decay angle) of $B^+\pi^-$ and $B^+\pi^+$ combinations.[1] The presence of the u quark in a B^+ meson implies the production of a $\bar{u}$ nearby in phase space. Ignoring strange hadron production and baryon production, this $\bar{u}$ will give rise to a π^- or a π^0; the remainder of the fragmentation chain, however, is charge symmetric, and one can expect equal production rates and kinematic properties for the $\pi^\pm$ produced there. While the inclusion of strange quarks, baryons, and excited $\bar{b}q$ states alter the details, it is useful to contrast the kinematic properties of the pion containing the anti-quark which is the partner of the light quark in the B meson (hereafter referred to as a *sister* pion, i.e. a close relative) with those of the other pions produced in the fragmentation process (hereafter referred to as *cousin* pions, i.e. more distant relatives). The results obtained on $B^+\pi^-$ and $B^+\pi^+$ correlations are used along with the assumption of isospin symmetry in the fragmentation of $\bar{b}$ quarks in Z^0 decays[6] to infer results for $B^0\pi^\pm$ correlations. Under isospin symmetry the multiplicity and kinematic properties of charged pions produced when a $\bar{b}$ fragments into a B^+ should be equal to those produced when a $\bar{b}$ fragments into a B^0 ($\bar{b}d$), including any structure due to resonant decays. The data can be used to test the validity of this assumption.

We also study the kinematic properties of B^+K^- and B^+K^+ combinations. The charge symmetry noted for Bπ combinations and the subsequent division into sister and cousin pions

[1] Charge conjugate processes are implied throughout this paper.

does not apply in the $B^+K^\pm$ system. Decays of $\bar{b}s$ combinations to non-strange B mesons will result in either B^+K^- or $B^0\bar{K}^0$, and the companion $\bar{s}$ will give rise to a K^+ or K^0.

The P-wave resonances referred to above would give rise to narrow structures in the invariant $B\pi$ mass distribution of sister pions via decays to $B^{(*)}\pi$ ($B^{(*)}\pi$ indicates the sum of $B\pi$ and $B^*\pi$). Excited $\bar{b}s$ states decay to $B_s^{(*)}\gamma$ or $B^{(*)}K$ depending on the mass of the $\bar{b}s$ state. The masses of P-wave $\bar{b}s$ states are expected to be close to B^*K threshold [4]. The amount of B_s produced in Z^0 decays is therefore sensitive to the masses and production rates of excited $\bar{b}s$ mesons; knowledge of the B_s production rate is important in analyses of B_s-$\bar{B}_s$ oscillations at LEP.

2 Event selection and Monte Carlo description

2.1 OPAL detector

The OPAL detector has been described elsewhere [7], and will be described only briefly here. The central detector consists of three wire chambers: a large volume jet chamber which measures particle trajectories and ionization energy loss (dE/dx), a smaller vertex drift chamber, and a set of planar drift chambers surrounding the jet chamber, oriented to measure the z coordinate.[2] These detectors are operated in a pressure vessel at 4 bar. Between the pressure vessel and a beryllium beam pipe are two layers of silicon strip detectors [8]. In this analysis only information from the strips oriented parallel to the beam axis was used. The entire central detector is inside a uniform axial magnetic field of 0.435 T. The region outside the coil is instrumented with time-of-flight counters, and both the barrel and the endcap regions are instrumented with lead-glass electromagnetic calorimeters preceded by presamplers. The iron return yoke of the magnet is instrumented as a hadron calorimeter, and 4 layers of muon chambers are outside the iron.

2.2 Event selection

Hadronic Z^0 decays are selected using the criteria described in Ref. [9]. Charged tracks and electromagnetic clusters unassociated with any charged track are grouped into jets using a cone jet algorithm [10]. The primary event vertex is reconstructed using the charged tracks in the event along with knowledge of the average position and effective spread of the e^+e^- collision point.

The analysis is performed on data collected in the vicinity of the Z^0 peak from 1991 through 1994. A total of 3.5 million hadronic events satisfied the event selection criteria.

[2] The OPAL coordinate system is defined with positive z along the electron beam direction; θ and ϕ are the polar and azimuthal angles, respectively.

2.3 Description of the Monte Carlo

Monte Carlo events are used to compare with experimental distributions and calculate the efficiencies of the selection criteria. The JETSET 7.3 Monte Carlo program [11, 12] was used to generate $Z^0 \to q\bar{q}$ decays which were processed by the detector simulation program [13]. Despite the detailed detector simulation it was necessary to degrade the curvature, angle, and impact parameter resolution on charged tracks produced in the Monte Carlo by an additional 30% to reproduce the resolutions observed in the OPAL data. This additional smearing was varied between 0 and 60% when evaluating systematic errors. The fragmentation is parameterized using the fragmentation function of Peterson *et al.*, [14] with $\epsilon_b = 0.0057$ and $\epsilon_c = 0.046$ in accordance with measurements of the mean energy fractions in $Z^0 \to b\bar{b}$ and $Z^0 \to c\bar{c}$ decays [15]. All weakly decaying b hadrons were generated with equal lifetimes. The B meson lifetimes in all Monte Carlo samples were reweighted to 1.6 ps, and the weakly decaying b baryon lifetimes to 1.2 ps. None of the standard Monte Carlo samples included production of P-wave mesons, neither in charm or beauty fragmentation nor in the charm mesons resulting from the decay of b hadrons. The effects of including these states are investigated using smaller samples of $Z^0 \to b\bar{b}$ events with P-wave states included. These samples were put through a faster, less detailed simulation which, nevertheless, provides a good description of the charged track acceptance and resolution.

3 Inclusive B reconstruction

The inclusive reconstruction of b hadrons starts with a jet in which a secondary vertex has been found. The following sections describe the secondary vertex selection and the estimators for the b hadron charge, direction and energy.

3.1 Vertex selection

The two highest energy jets in each event are searched for secondary vertices. Within each jet the vertexing algorithm takes the three tracks with the most significant separation from the primary vertex in the $r\phi$ plane as seed tracks and forms seed vertices from the crossing points of pairs of these tracks. Each seed vertex is considered in turn. A trial combination of each charged track in the jet with the seed vertex is made and the combination resulting in the vertex with the smallest χ^2 is retained, provided the χ^2 probability of the resulting vertex is at least 1%. The seed vertex parameters are updated and the process is iterated until there are no acceptable tracks to add. If several acceptable vertices are found in the same jet, the vertex with the largest number of assigned tracks is retained; if this choice is not unambiguous, the candidate vertex with the most significant separation from the primary vertex is chosen. Secondary vertex candidates are accepted if they contain at least 3 tracks, are separated from the primary vertex by at least 5 times the uncertainty in the separation distance as calculated using the vertex covariances, and if the output value of an artificial neural network designed to reject non-b background is acceptable.[3] The position of the primary vertex is then

[3]The neural network has 7 input parameters, the most important of which are the decay length, its uncertainty and the vertex multiplicity.

redetermined excluding tracks that were assigned to the secondary vertex. No attempt is made to find a separate decay vertex for the charm particle originating from the b hadron decay. Given the requirements described above the separation between the reconstructed vertex and the primary vertex is usually large compared to the separation between the true b and charm vertices.

The positions of the primary and secondary vertices are used to estimate the ϕ angle of the B hadron momentum vector. The calculated uncertainty in this angle, based on the vertex positions and covariances, is required to satisfy $\sigma_\phi < 0.015$ radians. At this stage there are 212 928 jets with reconstructed vertices satisfying these criteria.

3.2 B charge and momentum vector estimation

For each track in a jet containing an accepted secondary vertex a weight is calculated to assess the probability that the track came from the secondary vertex relative to the probability that it came from the primary vertex. A first estimate of the weight is given by

$$\omega' = \frac{R(b/\eta)}{R(b/\eta) + R(d/\sigma)} \ , \tag{1}$$

where R is a symmetric function describing the impact parameter significance with respect to a fitted vertex, b and η are the impact parameter and associated uncertainty in the $r\phi$ plane with respect to the secondary vertex, and d and σ are the same quantities with respect to the primary vertex. On average, more tracks come from the secondary vertex than from the primary in the events of interest, so ω' underestimates the probability that a track comes from the secondary vertex. This underestimate is most significant at higher momenta. A Monte Carlo simulation is used to correct ω' as a function of momentum. This new weight, ω, populates the range $[0, 1]$ and is used in all subsequent calculations.

Estimates of the b hadron momentum vector and charge are based on these weights. The charge estimate is given by the sum

$$q_{vtx} = \sum_{i=1}^{N_{jet}} \omega_i q_i \ , \tag{2}$$

where N_{jet} is the number of charged tracks in the jet and q_i is the charge of track i. The accuracy of the charge estimate provided by q_{vtx} can be gauged by its r.m.s.,

$$\sigma_q = \left(\sum_{i=1}^{N_{jet}} \omega_i (1 - \omega_i) q_i^2 \right)^{1/2} \ . \tag{3}$$

As a compromise between the number of selected vertices and the reconstructed charge resolution we require $\sigma_q < 0.8$. After applying this criterion, a sample of 84 693 vertices remain, from which the remainder of the analysis is performed. The predicted composition of the tagged vertex sample is given in Table 1. The selection criteria favor vertices from the decays of charged B hadrons due to the requirement that at least 3 charged tracks are assigned to the vertex. The non-b background comes predominantly from $Z^0 \to c\bar{c}$ events. There are 45 219 vertices satisfying $|q_{vtx}| > 0.6$.

Source	overall fraction	with $\|q_{vtx}\| > 0.6$
B^+	40 ± 3	54 ± 2
non-b background	11 ∓ 2	13 ∓ 2
All neutral b hadrons	49 ± 2	33 ± 1
- B^0	34	23
- B_s	9	6
- other b hadrons	6	4

Table 1: Predicted composition of the tagged vertex sample in percent. The calculation of the uncertainties is described in the text.

Figure 1 shows the overall q_{vtx} distribution for data and Monte Carlo. In this and all following figures, the Monte Carlo and data distributions are normalized to the same number of selected secondary vertices unless stated otherwise. This distribution can be used to check the sample composition predicted in the simulation. The charged B component and the non-b component have similar shapes and cannot readily be distinguished in the q_{vtx} distribution, but the neutral b hadron component has a markedly different shape. A fit to two components, charged B plus non-b background and neutral b hadron, yields a neutral b hadron fraction of 0.47 ± 0.01, which is slightly lower than the predicted value of 0.49; we assign an uncertainty of ± 0.02 to the neutral b hadron fraction. The uncertainty on the number of non-b background tags due to uncertainties in the modeling of the charged track resolution and in the production rates of charmed hadrons in $Z^0 \to c\bar{c}$ events is $\pm 20\%$. The total uncertainty on the B^+ fraction is obtained by adding in quadrature the uncertainties in the neutral b hadron fraction and in the non-b background.

We define the momentum vector of the charged particles coming from the b hadron decay as

$$\vec{p}_{vtx} = \sum_{i=1}^{N_{jet}} \omega_i \vec{p}_i \quad . \tag{4}$$

The $\vec{p}_{vtx}$ determined this way serves as an interim estimator for the B direction. All electromagnetic clusters unassociated with charged tracks that lie within 0.4 radians of $\vec{p}_{vtx}$ are scaled by 0.7 and summed to form the vector $\vec{p}_{EM}$. The scaling is done to account for neutral energy not associated with the B decay; the B energy resolution is not very sensitive to the value chosen. The direction of the b hadron is calculated using the ϕ angle defined by the vector from the primary vertex to the secondary vertex, and using the θ angle of the vector $\vec{p}_{vtx} + \vec{p}_{EM}$. The distribution of the difference between the reconstructed and generated ϕ of the b hadron in simulation can be described by a fit to two Gaussians. The sigma of the narrower Gaussian is 0.009 radians, and 84% of the entries lie within three sigma. The corresponding quantities describing the θ resolution are $\sigma = 0.014$ radians and 88%, respectively.

The resolution on the total energy of the b hadron candidate can be improved by more than a factor of two relative to the estimate provided by $\vec{p}_{vtx} + \vec{p}_{EM}$ if one includes the information that the total center of mass energy, E_{CM}, is twice the LEP beam energy. We calculate the total jet energy using this constraint and the recoil mass of the rest of the event:

$$E_{jet}^{tot} = \frac{E_{CM}^2 - m_{rec}^2 + m_{jet}^2}{2E_{CM}} \ , \tag{5}$$

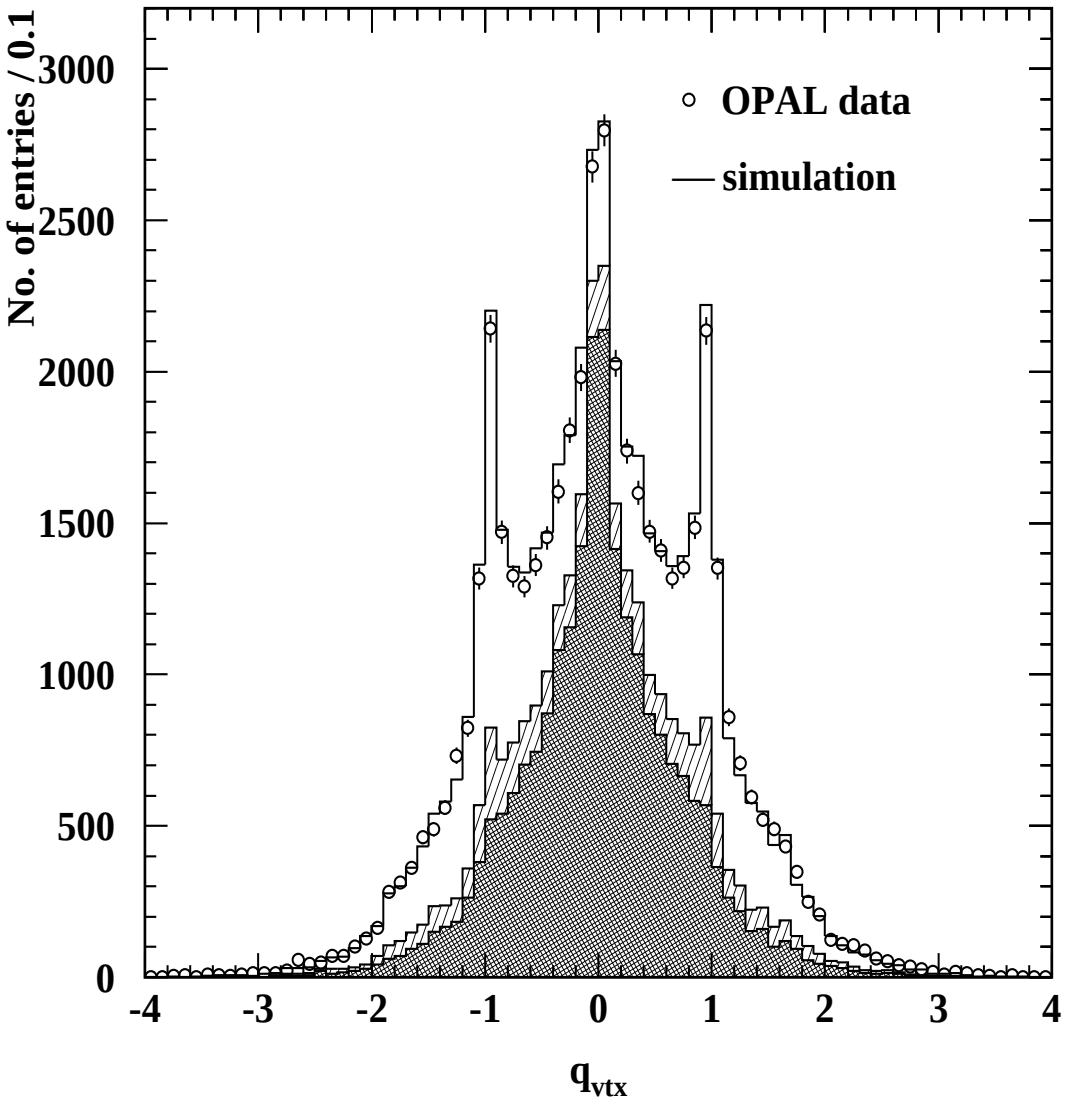

Figure 1: The distribution of q_{vtx} in the data (points) and the expectation from the simulation (histogram). The distributions are normalized to the same number of entries. The solid region shows the contribution from all neutral b hadrons, the hatched region shows the contribution from non-b events and the remaining contribution is from $B^{\pm}$.

where m_{rec} is the recoil mass calculated using charged tracks and unassociated electromagnetic clusters *outside* the jet, and m_{jet} is set to the B mass (the estimate is insensitive to the exact value used for m_{jet}). The b hadron energy estimate is this total energy minus the energy within the jet attributed to fragmentation:

$$E_B = E_{jet}^{tot} - (E_{jet}^{vis} - E_{vtx} - E_{EM}) \ , \tag{6}$$

where the visible jet energy E_{jet}^{vis} is the sum over all charged tracks and unassociated electromagnetic clusters in the jet, E_{vtx} is the energy of $\vec{p}_{vtx}$, and E_{EM} is the energy of $\vec{p}_{EM}$. In this calculation all charged particles are assigned the pion mass and all neutral clusters are taken as massless. The narrower Gaussian from a two Gaussian fit to the difference between

the reconstructed and generated b hadron energy has $\sigma = 2.8$ GeV, and 95% of the entries are contained within 3σ. The b hadron momentum is given by $\sqrt{E_B^2 - m_B^2}$, with m_B fixed to 5.279 GeV.

4 Study of Bπ correlations

Given a reconstructed b hadron momentum vector we search for pions originating from the primary event vertex. Pion candidates are rejected if they have no associated hits in the z drift chambers, if their measured $\mathrm{d}E/\mathrm{d}x$ is more than 2.58 standard deviations from the expected value for pions, if they have a total momentum less than 0.5 GeV or greater than 10 GeV, or if they have a secondary vertex weight, ω_π, greater than 0.2. With these requirements the simulation indicates that approximately 4.3% of the selected pions come from the weak decays of b hadrons, the remainder coming from the Z^0 decay point. The Bπ invariant mass is calculated as

$$m_{\mathrm{B}\pi} = \sqrt{m_B^2 + m_\pi^2 + 2E_B E_\pi - 2\vec{p}_B \cdot \vec{p}_\pi} \ , \tag{7}$$

with m_B fixed to 5.279 GeV. The mass resolution for Bπ combinations is a function of the Bπ − B mass difference. The resolution in a Monte Carlo sample for combinations whose true mass lies in the range 5.6–5.8 GeV has $\sigma = 35$ MeV, with 91% of the entries within $\pm 3\sigma$.

As a test of the mass resolutions predicted by the simulation we examine the Bγ mass spectrum. The inclusively reconstructed B candidates are combined with well-measured converted photons in the central detector, yielding the distribution shown in Figure 2.[4] The Bγ mass is calculated as in Eqn. 7 with m_π set to zero. The mass resolution is dominated by the uncertainties in the reconstructed B momentum vector. There is good agreement in the width of the peak indicating that the properties of the inclusively reconstructed B sample are well simulated. A simple Gaussian fit to the background subtracted peak gives a sigma of 5.5 MeV and a B* mass of 5.325 ± 0.001 GeV (statistical error only), in good agreement with the measured value, 5.325 ± 0.002 GeV [16].

The distribution of the product of the pion and vertex charges, $q_\pi q_{vtx}$, is used to subdivide the Bπ sample into like-sign and unlike-sign samples. This quantity has a slight negative bias (0.11 units) for both charged and neutral b hadrons. The bias can be understood as follows. A negative (positive) track from the primary vertex with a large value of ω will cause q_{vtx} to be too negative (positive). The tracks surviving the cut $\omega_\pi < 0.2$ will be more likely to be positive (negative), since the negative (positive) track with large ω will fail this cut. The mean of $q_\pi q_{vtx}$ thus acquires a negative bias. This bias is reduced as the cut on σ_q is lowered.

Accounting for this bias, we define the unlike-sign sample as those Bπ combinations with $q_\pi q_{vtx} < -0.71$, and the like-sign sample as those combinations with $q_\pi q_{vtx} > 0.49$. Having accounted for the bias with these asymmetric requirements, we expect processes producing equal numbers of Bπ^+ and Bπ^- to contribute equally to the two samples. These Bπ mass distributions are shown in Figures 3a and 3b for data (points) and for a Monte Carlo simulation with no resonant Bπ production (histogram).

[4] The acceptance for photon conversions as a function of the energy of the e^+e^- pair in the simulation was adjusted so as to bring the distributions of the number of conversions versus energy in the data and simulation into agreement.

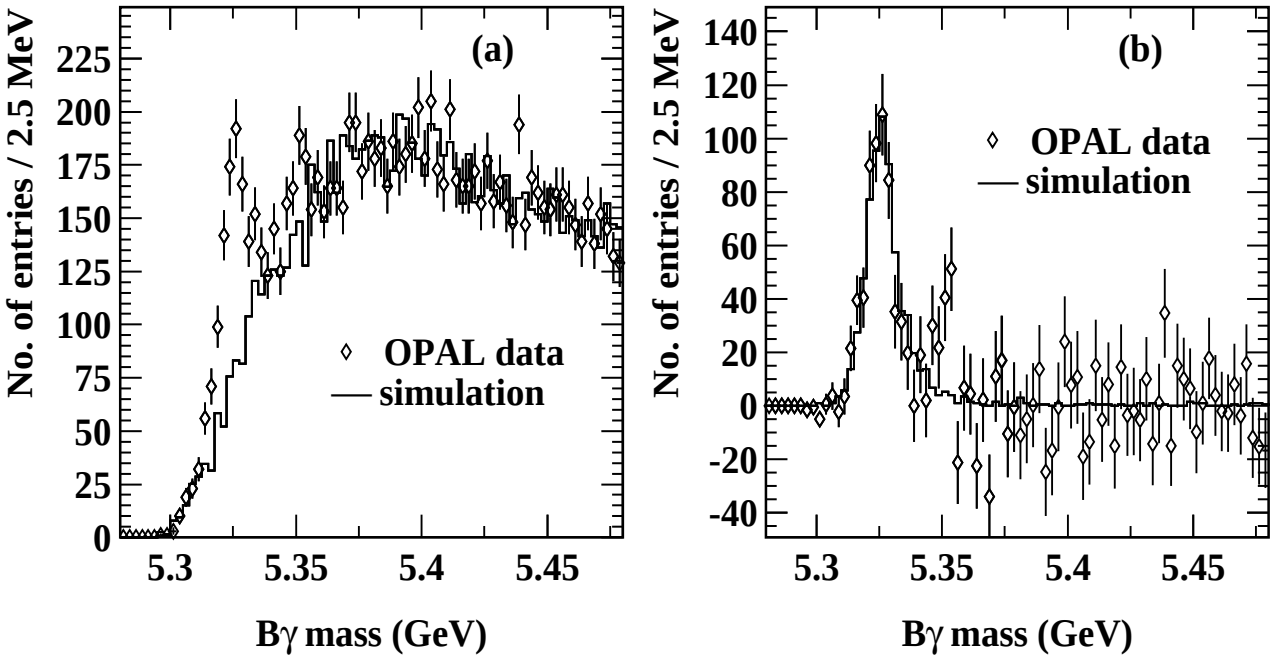

Figure 2: The reconstructed Bγ invariant mass using converted photons is shown as the points in (a). The histogram shows the shape of the combinatorial background predicted by the simulation. Subtracting this estimated background from the data yields the open points in (b), where the histogram shows the distribution for true $B^* \to B\gamma$ decays in the simulation.

The sister and cousin pion distributions are obtained from the observed unlike-sign and like-sign distributions. If the tagged vertex sample contained only B^+ with correct charge assignment, the like-sign distribution would itself be the cousin pion distribution, and the sister pion distribution would be obtained simply by subtracting the like-sign distribution from the unlike-sign distribution. The presence of other b hadrons, however, complicates matters. In particular mis-tagged B^0 will contribute to both sign combinations, so both the unlike-sign distribution and the like-sign distribution will include some sister pions associated with B^0. The sister pion distribution for B^+ can still be obtained by subtracting like-sign from unlike-sign, since the contributions from the neutral b hadrons are charge symmetric. Assuming isospin invariance for Bπ combinations, the sister pions in the like-sign distribution can be removed. The cousin pion distribution is obtained by subtracting from the like-sign distribution the unlike-sign distribution multiplied by a scale factor. This scale factor is the ratio of the number of $B^+\pi^-$ and $B^0\pi^+$ combinations in the like-sign sample to the number of $B^+\pi^-$ and $B^0\pi^+$ combinations in the unlike-sign sample, and is calculated in the simulation to be 0.21 ± 0.02, where the uncertainty comes from varying the bias used in defining the $q_\pi q_{vtx}$ cuts by ± 0.03.

The sister and cousin pion distributions obtained in this manner in data and simulation are shown in Figures 3c and 3d, respectively. These plots suggest that the Monte Carlo modeling of the fragmentation process is quite reasonable for the cousin pions, but that the simulation is missing a component with a mass near 5.7 GeV for the sister pions. The structure observed in Figure 3c will be further discussed in Section 7.

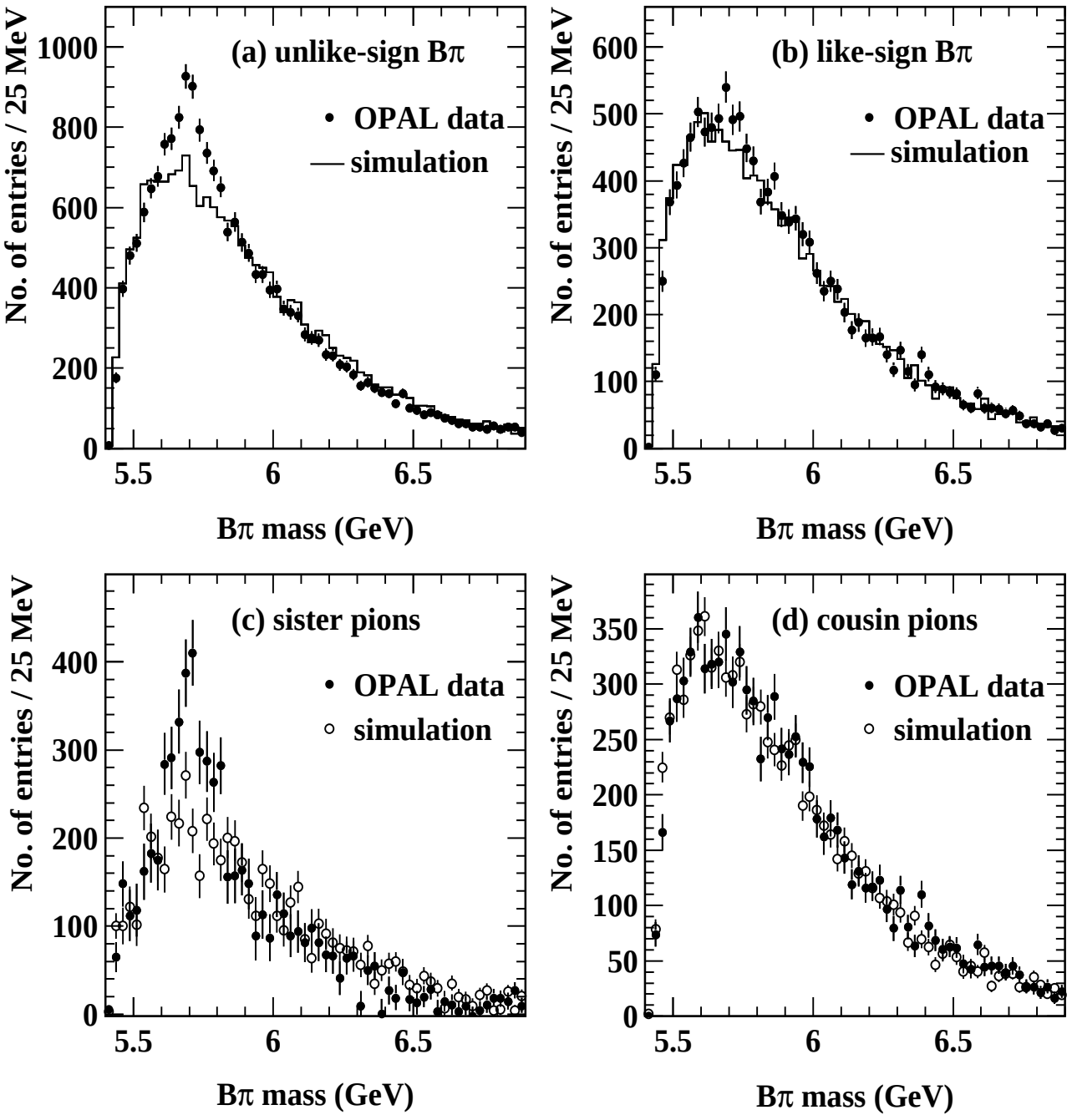

Figure 3: The reconstructed Bπ invariant mass distributions for unlike-sign combinations (a) and like-sign combinations (b). The points are the data and the histogram is from a Monte Carlo simulation with no resonant Bπ production, normalized to the same number of secondary vertices. The distributions for sister pions (c) and cousin pions (d) are described in the text.

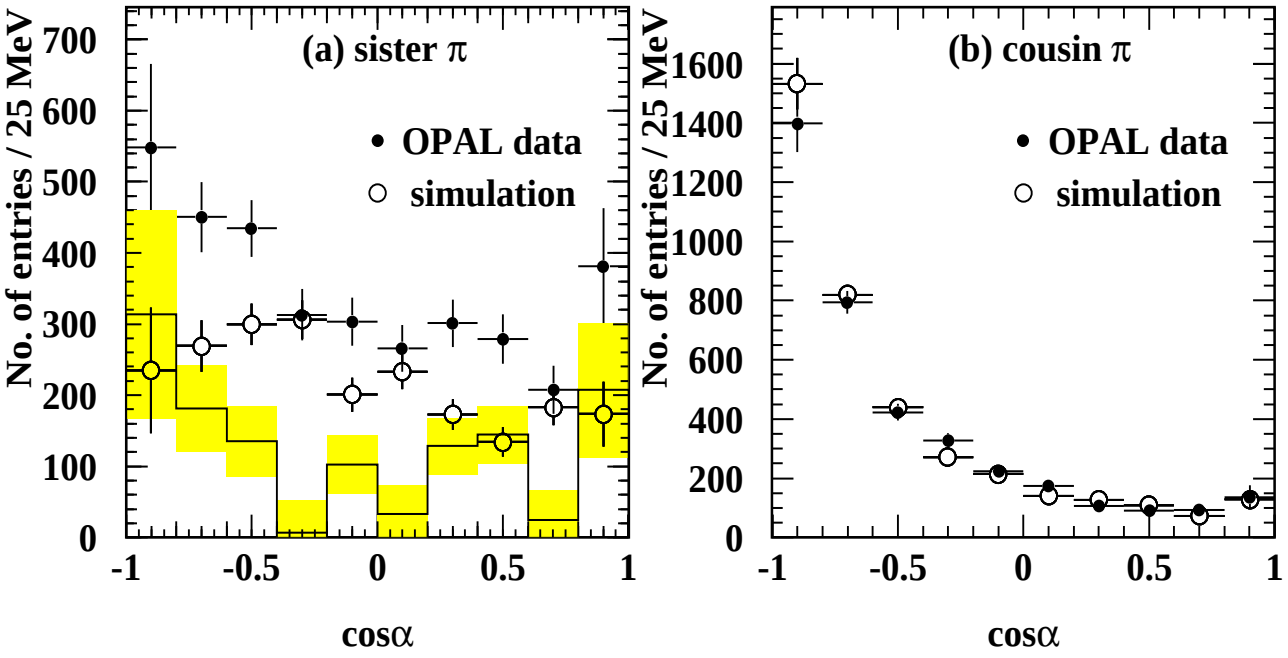

Figure 4: The efficiency corrected distributions of the cosine of the angle α (described in the text) for "sister" pions (a) and "cousin" pions (b) in data (solid points) and simulated events with no resonant Bπ production (open points). Only combinations with Bπ invariant mass between 5.60 and 5.85 GeV are plotted. The histogram in (a) shows the difference between the data and simulation, and the shaded area indicates the associated statistical errors.

Figures 4a and 4b show the distributions of $\cos\alpha$ for sister and cousin pions, where α is the helicity angle of the pion in the Bπ rest frame relative to the direction of flight of the Bπ system in the lab frame. Pions giving Bπ masses between 5.60 and 5.85 GeV are plotted after correcting for the efficiency of the pion selection requirements as a function of $\cos\alpha$. The solid points are data and the open points are from simulated events. The distribution of the excess sister pions in the data with respect to the Monte Carlo prediction, shown as the histogram in Figure 4a, is consistent with being isotropic.

5 Flavor tagging with associated pions

The rate at which pions can be used to tag the initial B^0 flavor and the purity of the flavor determination are of interest in evaluating the usefulness of Bπ correlations for CP violation studies involving neutral B mesons. We can study the ability of associated pions to tag the flavor of $B^{\pm}$ directly; the results for B^0 flavor tagging are identical under the assumption of isospin invariance. As seen in Figure 4, the distributions of sister pions and cousin pions in $\cos\alpha$ are markedly different (recall that the charge of sister pions is correlated with the B flavor, while the charge of cousin pions is not). This allows the selection of a useful region for b flavor tagging. The data in the region $5.60 < m_{\mathrm{B}\pi} < 5.85$ GeV and $\cos\alpha > -0.7$ show a

marked enhancement of sister pions relative to cousin pions. Defining pion tags as those which satisfy these criteria[5], we observe 5 749 (3 221) pion tags with charge sign opposite to (the same as) the reconstructed b hadron. To extract the rate and purity for flavor tagging with these pions the contributions to the $B\pi$ distributions from neutral b hadrons and from non-b events must be subtracted. Contributions from B_s, b baryons and non-b events are removed based on the predictions of the simulation. The B^0 contribution can be subtracted without using any information about $B\pi$ correlations from the simulation by noting that $B^0\pi^\pm$ combinations contribute equally to the like-sign and unlike-sign samples and by assuming isospin invariance for $B\pi$ combinations. Correcting for the efficiency of the pion selection criteria and dividing by the number of B^+ available, the rate at which pion tags are produced is

$$\frac{b \to (B^+\pi^\pm)_{\rm tag}}{b \to B^+} = 0.39 \pm 0.03 \ , \tag{8}$$

and the probability that the pion charge correctly tags the B^+ flavor is 0.706 ± 0.013.

Removing the cut on the $B\pi$ invariant mass increases the efficiency for tagging the b flavor with only a small increase in the mis-tag rate. Requiring only $\cos\alpha > -0.7$ and proceeding through the calculation described above, we find that pion tags are produced for 0.83 ± 0.06 of the B^+ candidates, and that the probability of inferring the B flavor correctly is 0.682 ± 0.012.

In an experiment where B^0 mesons are fully reconstructed one can expect a high efficiency for reconstructing the associated charged pion. Assuming this additional efficiency to be 90% yields a figure of merit for CP asymmetry measurements, namely the product of the efficiency times the square of the dilution due to flavor mis-tagging, of 0.06 (0.10) with the cut on $m_{B\pi}$ applied (removed). For comparison, figures of merit for lepton-based tags of the initial B flavor (based on tagging the flavor of the other b hadron in the event) are typically ≈ 0.03. While the situation may be different for B mesons produced in other environments (e.g. at a hadron collider), at LEP b flavor tagging using charged pions has greater statistical power than using semileptonic decays of the other b hadron in the event.

6 Study of BK correlations

In analogy with the $B\pi$ case, we study BK combinations as a function of $q_K q_{vtx}$. The kaon candidate is required to have associated hits in the z drift chambers, a momentum above 2 GeV to ensure good π-K separation in dE/dx, a measured dE/dx less than 2 standard deviations from the expected value for kaons and more than 2 standard deviations from the expected value for pions, and $\omega_K < 0.4$. The cut on ω is relaxed to increase the efficiency. Monte Carlo studies suggest that $\approx 8\%$ of the kaons selected in this manner originate from the weak decays of B hadrons and cascade charm decays. The pion contamination in the kaon candidate sample is estimated to be 10% in the simulation, and the proton contamination to be 30%. The distribution of reconstructed minus generated mass for BK combinations with generated masses in the range 5.80–5.96 GeV has $\sigma = 30$ MeV, with 93% of the entries within $\pm 3\sigma$. The BK mass distributions are shown in Figure 5. The like-sign distribution is well modeled in the simulation, whereas the unlike-sign distribution in the data shows an excess at low BK masses.

[5] If there is more than one pion tag for the same reconstructed b hadron, the charge of the tag with the largest value of $\cos\alpha$ is taken.

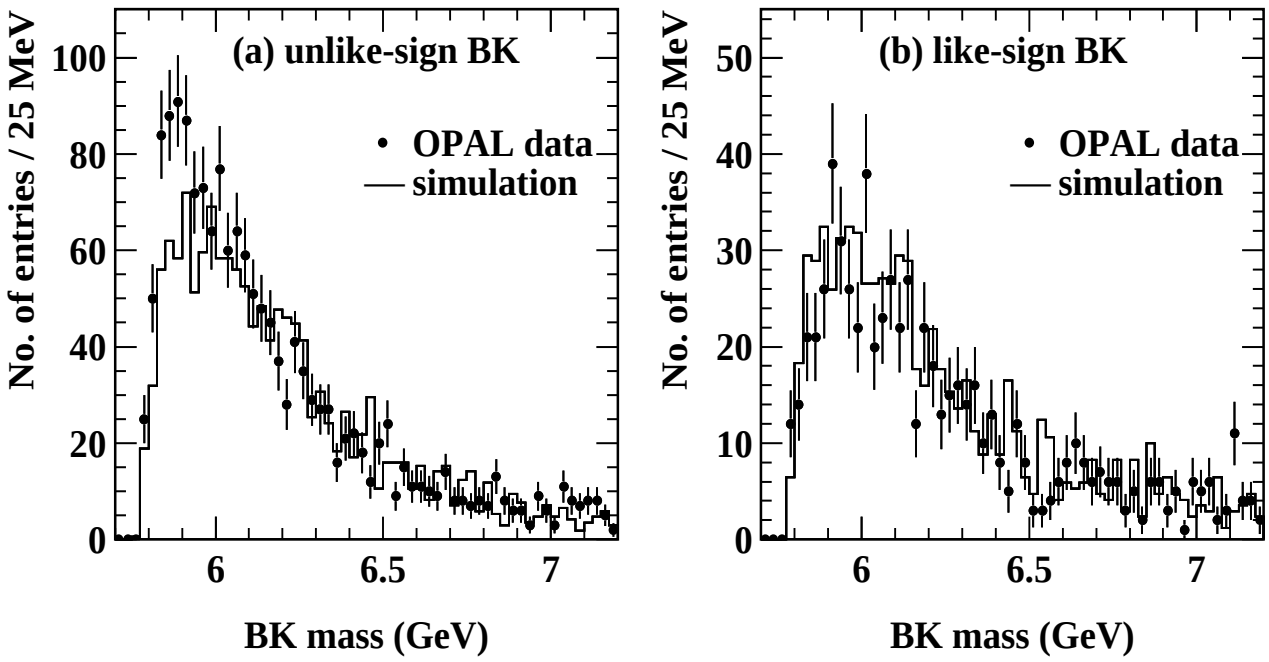

Figure 5: Reconstructed BK invariant mass distributions for unlike-sign combinations (a) and like-sign combinations (b). The points are the data and the histogram is from a Monte Carlo simulation with no resonant BK production, normalized to the same number of B vertices.

The possible reflection of the observed Bπ peak into the BK distribution was considered. The number of pions from the Bπ excess that reflect to the mass region of the BK excess is calculated to be 8 ± 2, which corresponds to about 5% of the observed excess.

7 Excited B meson production

7.1 Resonant Bπ production

The enhancement near 5.7 GeV in the sister pion Bπ mass distribution (Figure 3c) suggests Bπ resonance production. Even in the presence of excited B mesons decaying to $B^{(*)}\pi$ the sister pion distribution will contain a significant number of pions from non-resonant fragmentation. Given the good agreement observed for cousin pions, we make the assumption that the Bπ mass distribution of those sister pions not coming from Bπ resonances can be described by the sister pion distribution in the simulation.[6] Resonant decays are expected to populate small Bπ masses, so we normalize the non-resonant shape from the simulation to the number of sister pions observed with $m_{B\pi} > 6.2$ GeV. The number of sister pions per secondary vertex in this normalization region in the data is 0.62 ± 0.08 of the number in the simulation. Subtracting the sister pions in the simulation from those in the data yields the distribution shown in Figure 6a.

[6] We note that there may be other contributions to the sister pion distribution in the data, e.g. broad, higher mass resonances, that may alter the shape.

The distribution shows a prominent peak near 5.7 GeV. A fit to a single Breit-Wigner resonance convoluted with detector resolution yields a mass of 5.681 ± 0.011 GeV and an intrinsic width $\Gamma = 0.116 \pm 0.024$ GeV. The peak is thus too broad to come from a single state of small intrinsic width. The fit is performed including a linear background to allow for uncertainties in the simulated background shape. The number of excess sister pions, $1\,738 \pm 121$, in the region $5.60 < m_{\mathrm{B}\pi} < 5.85$ GeV serves as our estimate of the enhancement. The number of fitted background events in this region is 153, which we take as an estimate of the systematic error on the number of excess sister pions.

The rate of the excess is determined by dividing by the efficiency, 0.42 ± 0.07, for the pion selection criteria, correcting for the leakage of $\mathrm{B}^+\pi^-$ combinations into the like-sign distribution (3.6%), and dividing by the number of B^+ vertices with $|q_{vtx}| > 0.6$. We find

$$\frac{\mathrm{BR}(\bar{\mathrm{b}} \to \mathrm{B}^{**} \to \mathrm{B}^{(*)+}\pi^-)}{\mathrm{BR}(\bar{\mathrm{b}} \to \mathrm{B}^+)} = 0.180 \pm 0.012(\mathrm{stat}) \pm 0.035(\mathrm{syst}) \ , \tag{9}$$

where B^{**} indicates the resonant state(s) giving rise to the observed excess between 5.60 and 5.85 GeV. The efficiency for the pion selection was determined assuming an isotropic $\cos\alpha$ distribution (see Figure 4a); the results obtained when assuming a $1 + 3\cos^2\alpha$ distribution are used to evaluate the systematic error. This variation dominates the systematic error on the branching ratio. Variations due to other selection efficiencies and to uncertainties in the tagged vertex sample and charge bias are in each case smaller than 5% in relative terms. If the observed enhancement is due to the strong decay of one or more excited $\bar{\mathrm{b}}\mathrm{d}$ states, the decay branching ratios should respect isospin symmetry. Thus $\mathrm{BR}(\mathrm{B}^{**} \to \mathrm{B}^{(*)+}\pi^-) \leq 2/3$, which implies

$$\frac{\mathrm{BR}(\bar{\mathrm{b}} \to \mathrm{B}^{**0})}{\mathrm{BR}(\bar{\mathrm{b}} \to \mathrm{B}^+)} \geq 0.270 \pm 0.056 \ . \tag{10}$$

In the presence of low-mass $\mathrm{B}\pi$ resonances, some sister pions[7] are shifted to low $\mathrm{B}\pi$ masses. The relative normalization given above of data and simulation in the region $m_{\mathrm{B}\pi} > 6.2$ GeV is consistent with expectations based on the resonant rate derived here.

7.2 Resonant BK production

The result of subtracting the prediction of the simulation from the observed BK mass distribution for unlike-sign pairs (Figure 5a) is shown in Figure 6b. The observed structure suggests resonant decays of excited $\bar{\mathrm{b}}\mathrm{s}$ states. Fitting the enhancement to a single Breit-Wigner resonance convoluted with detector resolution on a linear background yields a mass of 5.853 ± 0.015 GeV and an intrinsic width $\Gamma = 0.047 \pm 0.022$ GeV. Defining the enhancement region as $5.80 < m_{\mathrm{BK}} < 6.00$ GeV results in 149 ± 30 combinations. The number of events in the signal region attributed to background by the fit, -6.8, is taken as an estimate of the systematic error on the number of excess $\mathrm{B}^+\mathrm{K}^-$ combinations.

The efficiency for selecting the kaon is 0.24 ± 0.04, using the same assumptions about the decay angular distribution as for the pion case. The derived production rate is

$$\frac{\mathrm{BR}(\bar{\mathrm{b}} \to \mathrm{B}_\mathrm{s}^{**} \to \mathrm{B}^{(*)+}\mathrm{K}^-)}{\mathrm{BR}(\bar{\mathrm{b}} \to \mathrm{B}^+)} = 0.026 \pm 0.005(\mathrm{stat}) \pm 0.006(\mathrm{syst}) \ , \tag{11}$$

[7] Recall that sister pions are obtained from the difference between the $\mathrm{B}^+\pi^-$ and $\mathrm{B}^+\pi^+$ distributions

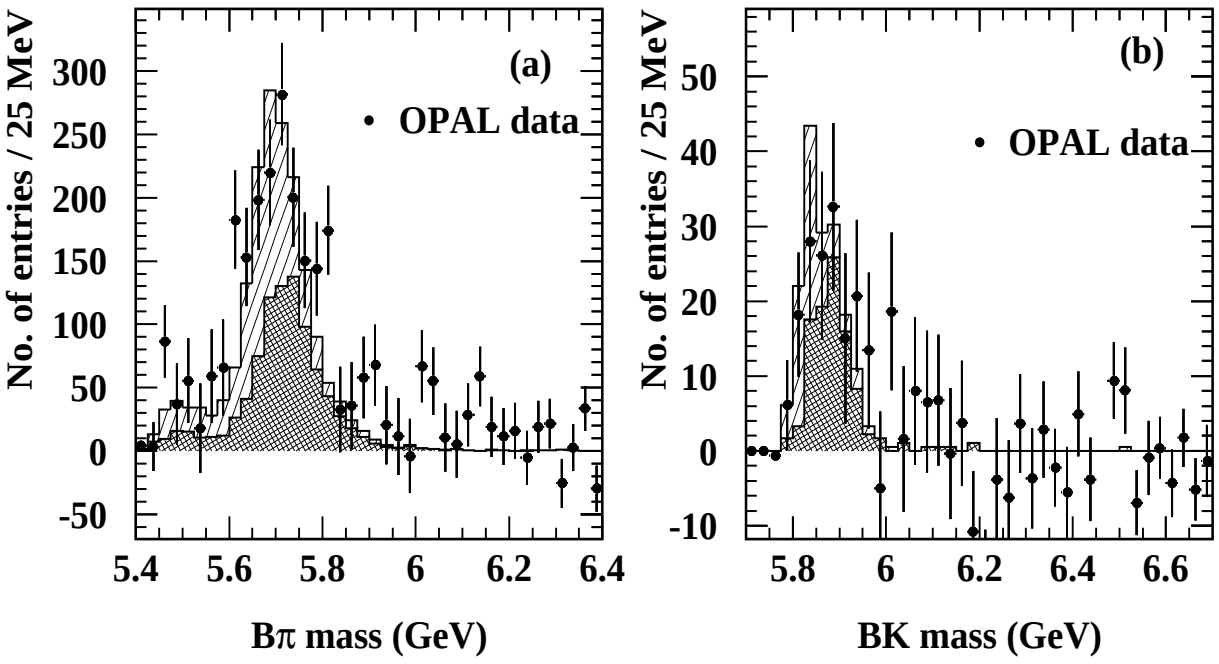

Figure 6: The Bπ invariant mass distribution for sister pions after subtracting the component expected from non-resonant combinations is shown in (a). The normalization of the data and simulation was done in the region above 6.2 GeV. The solid histogram shows the contribution from the B_2^* state generated with the parameters of Table 2, and the hatched histogram shows the contribution from the B_1 state. The B^+K^- invariant mass, after subtracting the distribution from a simulation without BK resonances, is plotted in (b). The solid and hatched histograms show the B_{s2}^* and B_{s1} states generated using the parameters of Table 2.

	B_1	B_2^*	B_{s1}	B_{s2}^*
Mass (GeV)	5.725	5.737	5.874	5.886
Width (GeV)	0.020	0.025	0.001	0.001
BR($B^+\pi^-/K^-$)	0.000	0.300	0.000	0.300
BR($B^{*+}\pi^-/K^-$)	0.533	0.300	0.500	0.200
BR($B^+\pi^0\pi^-$)	0.100	0.007		
BR($B^{*+}\pi^0\pi^-$)	0.033	0.060		

Table 2: Generated parameters of P-wave B mesons.

where B_s^{**} indicates the resonant state(s) giving rise to the observed excess between 5.80 and 6.00 GeV. The systematic error is again dominated by the uncertainty in the distribution of the decay angle; changing the nominal charge bias assumed in the data (0.11) by ± 0.03 changes the rate by $\pm 12\%$, and all other sources of uncertainty contribute less than 5% relative error.

If the observed enhancement is due to the strong decay of one or more excited $\bar{b}s$ states, the decay branching ratios should respect isospin symmetry. Thus $BR(B_s^{**} \to B^{(*)+}K^-) \leq 1/2$. To compare the ratio of B_s^{**} to pseudoscalar B_s we assume 0.3 $\bar{b}s$ are produced for each $\bar{b}d$. This implies

$$\frac{BR(\bar{b} \to B_s^{**0})}{BR(\bar{b} \to B_s)} \geq 0.175 \pm 0.052 \ . \tag{12}$$

The excess B^+K^- pairs indicate that some $\bar{b}s$ combinations result in non-strange pseudoscalar B mesons in the data. The $\bar{b}s$ combinations in the simulation used here produce only B_s and B_s^*. Incorporating strongly decaying $\bar{b}s$ states in the simulation would reduce the number of B_s generated.

7.3 Comparison with expectations for P-wave states

The distributions expected for simulated decays of the B_1 and B_2^* states, using the parameters indicated in Table 2, are overplotted in Figure 6a, and those for B_{s1} and B_{s2}^* in Figure 6b. These values are similar to those proposed in [4], but the masses of the B_1 and B_2^* states have been decreased by 30 MeV, and those of the B_{s1} and B_{s2}^* states raised by 40 MeV. The two spin states have been assumed in each case to have equal production rates; recent measurements [3] of D_1 and D_2^* in e^+e^- annihilations at $\sqrt{s} = 10.6$ GeV suggest equal production rates in the charm sector. Note that the $B\pi$ mass calculated from Eqn. 7 is shifted downward by 47 MeV when the transition is to B^*. This shifts the B_1 peak and effectively broadens the B_2^* peak, since B_2^* decays to both $B\pi$ and $B^*\pi$. These P-wave mesons provide a qualitative explanation for the observed enhancements.

7.4 Neutral b hadrons

The rates derived for $B\pi$ correlations assume isospin symmetry for $B\pi$ combinations. This assumption can be tested by considering the invariant mass distribution of $B\pi$ combinations satisfying $-0.71 < q_\pi q_{vtx} < 0.49$, shown in Figure 7a. If the excess seen in Figure 3a was due solely to $B^+\pi^-$ combinations, one would expect only 42% as many excess events in Figure 7a; if the production is isospin symmetric, one expects roughly equal populations of excess events in these two plots. The ratio of the excess $B\pi$ combinations seen in the signal region ($5.60 < m_{B\pi} < 5.85$ GeV) in Figure 7a to those seen in Figure 3a is 0.79 ± 0.13, supporting the assumption of isospin symmetry.

The distribution of BK invariant masses for combinations with $-0.71 < q_K q_{vtx} < 0.49$ is shown in Figure 7b. In contrast to the unlike-sign BK combinations in Figure 5a, no peak near threshold is observed in this case. The decays of $\bar{b}s$ states just above BK threshold proceed to B^+K^- and $B^0\bar{K}^0$, the latter of which would not produce an enhancement in this distribution.

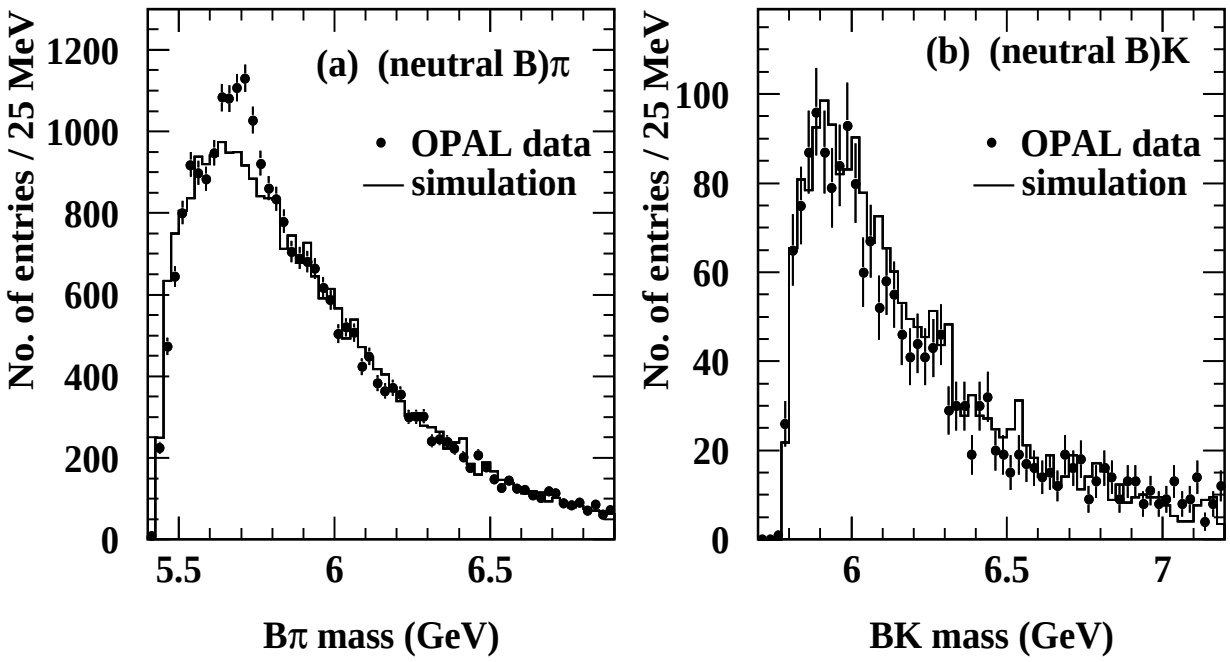

Figure 7: Reconstructed Bπ (a) and BK (b) invariant mass distributions for combinations with $-0.71 < q \cdot q_{vtx} < 0.49$. The points are the data and the histogram is from a Monte Carlo simulation with no resonant Bπ or BK production, normalized to the same number of secondary vertices.

We therefore expect only a contribution from excess B^+K^- combinations where the measured charge of the B^+ is close to zero. In addition, we expect the simulation to overestimate the contribution in Figure 7b from $B_sK^\pm$ combinations,[8] as was discussed in Section 7.2. However, the relatively low statistics in Figure 7b and other uncertainties, including the contamination of the kaon sample by misidentified protons, prevent quantitative tests of these expectations.

8 Conclusion

We have observed substantial correlations between B meson flavor and pion charge for Bπ combinations where the decay angle of the pion in the Bπ rest frame satistfies $\cos\alpha > -0.7$. The charge of pions in this kinematic region has been shown to provide a useful method for tagging the $B^\pm$ flavor. Assuming the Bπ combinations respect isospin symmetry, we conclude that associated pions can provide a tag of initial B^0 flavor that compares favorably with lepton-based flavor tags.

We also observe enhancements in the invariant mass distributions of unlike-sign Bπ and BK combinations. The enhancement observed in B^+K^- signals a suppression of pseudoscalar B_s meson production in Z^0 decays. The enhancement observed in $B^+\pi^-$ is too broad to be

[8] While B_s are produced less frequently than B^0, requiring a kaon from the primary vertex enhances their contribution in Figure 7b.

due to a single state of small intrinsic width. While we cannot unambiguously identify these enhancements with particular resonant states, they are consistent with the picture of P-wave resonances of light quarks and b antiquarks. We estimate that the production of B mesons in $Z^0 \to b\bar{b}$ decays proceeds via these excited states more than 20% of the time.

Acknowledgements:

It is a pleasure to thank the SL Division for the efficient operation of the LEP accelerator, the precise information on the absolute energy, and their continuing close cooperation with our experimental group. In addition to the support staff at our own institutions we are pleased to acknowledge the
Department of Energy, USA,
National Science Foundation, USA,
Particle Physics and Astronomy Research Council, UK,
Natural Sciences and Engineering Research Council, Canada,
Fussefeld Foundation,
Israel Ministry of Science,
Israel Science Foundation, administered by the Israel Academy of Science and Humanities,
Minerva Gesellschaft,
Japanese Ministry of Education, Science and Culture (the Monbusho) and a grant under the Monbusho International Science Research Program,
German Israeli Bi-national Science Foundation (GIF),
Direction des Sciences de la Matière du Commissariat à l'Energie Atomique, France,
Bundesministerium für Forschung und Technologie, Germany,
National Research Council of Canada,
A.P. Sloan Foundation and Junta Nacional de Investigação Científica e Tecnológica, Portugal.

References

[1] M. Gronau, A. Nippe, and J. L. Rosner, Phys. Rev. **D 47**, (1993) 1988.

[2] ARGUS Collaboration, H. Albrecht *et al.*, Phys. Lett. **B 221** (1989) 422; **B 231** (1989) 208; **B 232** (1989) 398;
Fermilab E691 Collaboration, J. C. Anjos *et al.*, Phys. Rev. Lett. **62** (1989) 1717;
CLEO Collaboration, P. Avery *et al.*, Phys. Rev. **D 41**, (1990) 774;
Fermilab E687 Collaboration, P.L.Frabetti *et al.*, Phys. Rev. Lett. **72** (1994) 324.

[3] CLEO Collaboration, P. Avery *et al.*, Phys. Lett. **B 331** (1994) 236.
CLEO Collaboration, T. Bergfeld *et al.*, Phys. Lett. **B 340** (1994) 194.

[4] The predictions for P-wave mesons used in this draft come from
E. J. Eichten, C. T. Hill, and C. Quigg, Phys. Rev. Lett. **71** (1993) 4116.
Some updated predictions by the same authors are available in "Orbitally Excited Heavy-Light Mesons Revisited," FERMILAB-CONF-94/118-T, May 1994.

[5] See, e.g., W. A. Bardeen and C. T. Hill, Phys. Rev. **D 49**, (1994) 409.

[6] I. Dunietz and J. L. Rosner, FERMILAB-PUB-94/298-T, October 1994. This preprint on "Isospin considerations in correlations of pions and B mesons" appeared after the analysis presented in this paper was essentially complete.

[7] OPAL Collaboration, K. Ahmet *et al.*, Nucl. Inst. and Meth. **A 305** (1991) 275.

[8] P. P. Allport *et al.*, Nucl. Inst. and Meth. **A 324** (1993) 34.
P. P. Allport *et al.*, Nucl. Inst. and Meth. **A 346** (1994) 476.

[9] OPAL Collaboration, G. Alexander *et al.*, Z. Phys. **C 52** (1991) 175.

[10] OPAL Collaboration, R. Akers *et al.*, Z. Phys. **C63** (1994) 197.
The maximum half-angle of the cone was set to 0.65 radians.

[11] T.Sjöstrand, Comp. Phys. Comm. **39** (1986) 347;
M. Bengtsson and T. Sjöstrand, Comp. Phys. Comm. **43** (1987) 367;
M. Bengtsson and T. Sjöstrand, Nucl. Phys. **B 289** (1987) 810;
T. Sjöstrand, CERN-TH/92-6488;
JETSET 7.4 is described in T. Sjöstrand, CERN-TH/93-7112.

[12] Parameter values were tuned to describe global event shape variables:
OPAL Collaboration, M. Akrawy *et al.*, Z. Phys. **C 47** (1990) 505.

[13] J.Allison *et al.*, Nucl. Inst. and Meth. **A 317** (1992) 47;

[14] C.Peterson, D.Schlatter, I.Schmitt and P.M.Zerwas, Phys. Rev. **D 27** (1983) 105.

[15] ALEPH Collaboration, Phys. Lett. **B 244** (1990) 551;
DELPHI Collaboration, Z. Phys. **C 56** (1992) 47;
L3 Collaboration, Phys. Lett. **B 261** (1991) 177;
OPAL Collaboration, Phys. Lett. **B 263** (1991) 311;
ALEPH Collaboration, Phys. Lett. **B 266** (1991) 218;
OPAL Collaboration, Z. Phys. **C 60** (1993) 199;
OPAL Collaboration, Phys. Lett. **B 262** (1991) 341;
OPAL Collaboration, Z. Phys. **C 60** (1993) 601.

[16] Particle Data Group, L. Montanet *et al.*, Phys. Rev. **D 50** (1994) 1175.